Journal of the Geological Society, *London*, Vol. **168**, 2011, pp. 333–347. doi: 10.1144/0016-76492010-067.

Origin of the Aves Ridge and Dutch–Venezuelan Antilles: interaction of the Cretaceous 'Great Arc' and Caribbean–Colombian Oceanic Plateau?

IAIN NEILL[1]*, ANDREW C. KERR[1], ALAN R. HASTIE[2], KLAUS-PETER STANEK[3] & IAN L. MILLAR[4]

[1]*School of Earth and Ocean Sciences, Cardiff University, Main Building, Park Place, Cardiff CF10 3YE, UK*

[2]*School of Geography, Geology and the Environment, Kingston University, Penrhyn Road, Kingston upon Thames KT1 2EE, UK*

[3]*Institut für Geologie, TU Bergakademie Freiberg, Bernhard-von-Cotta-Strasse 2, D-09596 Freiberg, Germany*

[4]*Natural Environment Research Council Isotope Geoscience Laboratories, Kingsley Dunham Centre, Keyworth NG12 5GG, UK*

**Corresponding author (e-mail: neilli@cardiff.ac.uk)*

Abstract: In this paper we reassess the geochronology and geochemistry of three dredge hauls from the SE corner of the Aves Ridge (Caribbean Sea) originally sampled in 1968 by Duke University's R.V. *Eastward*. Two hauls consist of light rare earth element-enriched granitoids with a U–Pb zircon emplacement age of 75.9 ± 0.7 Ma. A further haul contains mostly calc-alkaline island arc basaltic andesites of uncertain age. Petrological, trace element and isotopic constraints indicate that the granitoids have an oceanic crustal source and were formed by melting of the lower arc, oceanic or oceanic plateau crust. The mafic rocks formed by partial melting of an incompatible trace element-enriched mantle wedge, which was probably composed of mantle plume material. Both the dredged rocks and data from the Dutch–Venezuelan Antilles indicate a period of west-dipping underthrusting and subduction beneath, or close to, the Caribbean–Colombian Oceanic Plateau between *c*. 88 and *c*. 59 Ma, concurrent with collision of part of the plateau with northwestern South America. Constraints from the geochemistry and geochronology of offshore southern Caribbean arc and plateau rocks suggest that in the southern Caribbean there was no pre-existing west-dipping subduction system during formation of the Caribbean–Colombian Oceanic Plateau, whereas long-lived SW-dipping subduction in the northern Greater Antilles is more probable.

Supplementary material: Sample details, major and trace element data (file 1), cathodoluminescence images of analysed zircons (file 2) and whole-rock standards (file 3) are available at http://www.geolsoc.org.uk/SUP18438.

The extant Caribbean Plate, bounded by subduction and transform margins, is considered to represent an allochthonous region of Pacific crust that has overridden proto-Caribbean oceanic crust and moved into the region between North and South America from the Cretaceous to the present day (Fig. 1; e.g. Kerr *et al.* 2003; Pindell *et al.* 2006; Pindell & Kennan 2009). During its relative eastwards motion, the Caribbean Plate was thickened by eruption of mantle plume-derived lavas mostly at *c*. 94–88 Ma (Sinton *et al.* 1998; Kerr *et al.* 2003) to form the Caribbean–Colombian Oceanic Plateau (e.g. Kerr *et al.* 2003).

North and South America rifted apart in the Jurassic during the break-up of Pangaea, intimately associated with sea-floor spreading in the central Atlantic. Separation resulted in the formation of oceanic crust between the Americas during the Late Jurassic in the Gulf of Mexico and the proto-Caribbean seaway (reviewed by Pindell & Kennan 2009). On the western margin of the proto-Caribbean, an island arc system initiated during the Early Cretaceous, termed the 'Great Arc of the Caribbean' (*sensu* Burke *et al.* 1978; Burke 1988). Burke *et al.* (1978) and Burke (1988) proposed that the rocks of the Greater Antilles, Aves Ridge, Lesser Antilles and Dutch–Venezuelan Antilles (Fig. 1) represent a history of subduction at the eastern edge of the Pacific and then the Caribbean Plate following its isolation from the Pacific. However, some workers treat these components of the Great Arc as separate entities because they appear to have distinct tectonic histories and initiated as single arc systems at different times during the Cretaceous to Palaeogene (e.g. Wright & Wyld 2010). Most magmatism is thought to have ceased on the pre-Lesser Antilles subduction systems during the Palaeocene to Early Eocene as the Grenada Basin opened (Pindell & Barrett 1990; Speed & Walker 1991; Bird *et al.* 1999) and roll-back of the west-dipping proto-Caribbean subduction zone subsequently initiated the currently active Lesser Antilles arc (Aitken *et al.* 2010). The Cretaceous subduction systems accreted to North and South America (Kerr *et al.* 2003) whereas the Lesser Antilles subduction zone continues to facilitate the eastwards movement of the Caribbean Plate relative to the Americas along transpressive plate boundaries (Fig. 1).

The polarity of subduction, particularly on the Greater Antilles arc system during the Early Cretaceous, has been the topic of much debate. It has been argued that the relative dispositions and long-lived high-pressure metamorphic histories of arc assemblages in Cuba and Hispaniola suggest SW-dipping subduction of proto-Caribbean crust dating back to at least 125 Ma following a subduction polarity reversal event (e.g. Pindell & Barrett 1990; Pindell & Kennan 2009; Stanek *et al.* 2009; Escuder Viruete *et al.* 2010). An alternative hypothesis is that the Caribbean–Colombian Oceanic Plateau choked an east-dipping Greater

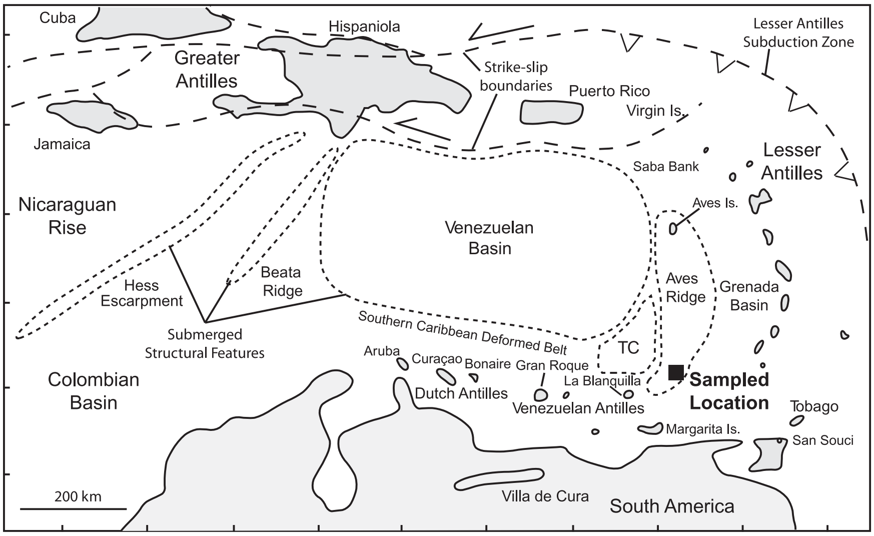

Fig. 1. Simplified map of the eastern Caribbean based on GEOMapApp (Haxby *et al.* 2010) showing the sampled location. Aruba, Curaçao and Bonaire make up the Dutch Antilles; Los Roques and La Blanquilla the Venezuelan Antilles; and Cuba, Jamaica, Hispaniola, Puerto Rico and the Virgin Isles the Greater Antilles. TC, thin crust of the southeastern Venezuelan Basin.

Antilles trench, forcing initiation of SW-dipping subduction during the Late Cretaceous (e.g. Burke 1988; Kerr *et al.* 2003; Thompson *et al.* 2003; Hastie & Kerr 2010).

In the southern Caribbean, the origin of the Dutch–Venezuelan Antilles (Fig. 1) is also contentious, as discussed by Wright & Wyld (2010) and van der Lelij *et al.* (2010). These workers showed that the Dutch–Venezuelan Antilles have a shorter geological history that is distinct from the Greater Antilles. In the Dutch–Venezuelan Antilles NW-dipping subduction began beneath the Caribbean–Colombian Oceanic Plateau at *c*. 88 Ma, and lasted until collision of the newly formed Dutch–Venezuelan Antilles arc with South America prior to the Campanian. Wright & Wyld (2010) argued that this subduction zone initiated at the southeastern margin of the Caribbean–Colombian Oceanic Plateau. In their model, island arc fragments that predate the Caribbean–Colombian Oceanic Plateau, such as those on Bonaire (Fig. 1), originated in a SW-dipping Greater Antilles arc and were transported southwards to their present locations by strike-slip motion. Alternatively, van der Lelij *et al.* (2010) proposed that the newly formed Caribbean–Colombian Oceanic Plateau collided with a pre-existing east-dipping subduction zone, causing a polarity reversal akin to the second model for the Greater Antilles outlined above.

The largely submerged Aves Ridge lies between the Dutch–Venezuelan Antilles and the Greater Antilles (Fig. 1). Most workers have argued that the Aves Ridge originated as a Late Cretaceous to early Palaeocene island arc (Bouysse 1984; Christeson *et al.* 2008; Pindell & Kennan 2009). However, the precise age, magmatic source(s) and subduction polarity of this arc are unclear. Given its significant spatial extent and because it is likely to represent some of the last island arc magmatism in the southeastern Caribbean prior to the opening of the Grenada Basin; a deeper understanding of the origin of the Aves Ridge could help to better constrain Caribbean Plate tectonic evolution.

In this paper we present new major and trace element and Nd and Hf isotopic analyses and new U–Pb zircon geochronological data from samples collected during dredging by R.V. *Eastward* in 1968. We use these results to determine the origin of the Aves Ridge. Data from the Aves Ridge and Dutch–Venezuelan Antilles are then combined to provide new constraints on models for the tectonic evolution of the southeastern Caribbean.

Geology of the Aves Ridge

Although the Aves Ridge is an extensive region of crust in the eastern Caribbean, the geochemistry of basement samples has not previously been studied in any detail. The ridge is a broadly north–south-trending arcuate structure *c*. 500 km in length, running between its sole emergent point at Aves Island in the Caribbean Sea and Margarita to the north of the Venezuelan coast (Fig. 1). The ridge has a topographic profile of up to 1500 m above the surrounding ocean basins and seismic studies reveal that the ridge has little sedimentary cover and a crustal thickness of *c*. 26 km (Christeson *et al.* 2008). Seismic velocities are >6.0 km s^{-1} in the mid-crust and *c*. 7.3 km s^{-1} at the base of the crust, consistent with an interpretation as a remnant island arc of intermediate composition (Clark *et al.* 1978; Christeson *et al.* 2008).

Glassy, brecciated basalts and andesites dredged or drilled from the northern end of the ridge and the Saba Bank between Aves Island and the Greater Antilles (Fig. 1) also suggest a volcanic arc origin (Marlowe 1968; Church & Allison 2004; Fig. 1). Dredge samples collected in 1968 by Duke University's R.V. *Eastward* are the only samples collected from the southern part of the ridge. Three dredges from the eastern scarp of the ridge (Fig. 1) contained significant quantities of igneous rocks and were described and dated by K–Ar methods by Fox *et al.* (1971). Dredge 11317 (12.30°N) contained 1500 kg of granitic boulders and pebbles. Four whole-rock K–Ar ages ranged from 57 to 89 Ma. Dredge 11318 (12.25°N) consisted of 40 kg of mostly doleritic cobbles and pebbles with lesser amounts of porphyritic and/or metamorphosed basalt, with two K–Ar ages of 57 and 60 Ma. Dredge 11319 (12.35°N) contained 2000 kg of granitoid material seemingly identical to dredge 11317, but with four K–Ar ages ranging from 18.5 to 67 Ma. No methods or errors were given for these K–Ar dates by Fox *et al.* (1971); however, the ages are unlikely to be reliable because of alteration, and this is evidenced by the wide spread of ages obtained.

Walker *et al.* (1972) showed that the granitoids had some primitive $^{87}Sr/^{86}Sr$ ratios, which ranged from 0.7038 to 0.7080. None the less, these ratios are likely to have been increased by interaction with Cretaceous seawater of $^{87}Sr/^{86}Sr$ *c*. 0.7075 (Veizer 1989) and/or hydrothermal alteration. No mafic rocks were found in the granitic dredges and vice versa. For this study, the largest, freshest blocks remaining from each dredge (tens of kilograms only) were selected from the Lamont–Doherty Earth Observatory Deep Sea Sample Repository in November 2008, generating 34 samples for analysis.

Petrology

Granitoids

The felsic rocks are coated in thick layers of manganese oxides, sometimes over 1 cm thick. The rocks are typically pink to pale green and slightly hydrothermally altered. Two facies have been identified within the granitoid samples. The dominant facies (*c*. 75%) is of a coarse, granitic nature and the other is fine-grained and more intermediate in composition. The primary mineralogy of the granitic rocks comprises plagioclase, quartz, alkali feldspar, hornblende and opaque minerals. The feldspars are sericitized and epidote is a common secondary mineral along with clays and chlorite. Zircon and titanite are the most common accessory minerals. Texturally, the rock is of a coarse interlocking nature, with grain sizes up to 2 mm and abundant interstitial quartz. Plagioclase is sometimes optically zoned and alkali feldspar is perthitic. Hornblende is squat or slightly elongate.

The intermediate facies occurs as isolated masses or clots distinct from the surrounding granitic material. The boundary between the two facies is, however, indistinct and gradational in thin section, suggesting that the darker clots may be restitic in nature. This second facies is dioritic and has a grain size ranging from 0.5 to 1 mm. The primary mineralogy is dominated by interlocking sericitized plagioclase, amphiboles, titanite and oxides. Only the dominant coarse granitic facies was selected for geochemical analysis, to avoid the generation of artificial mixtures of the two rock types.

Mafic rocks

The mafic rocks have undergone variable degrees of pervasive alteration. The freshest specimens from the small sample set were reserved for geochemical analysis so little solid rock remains. From the remaining rocks it can be seen that many have a fine-grained matrix that is composed of clay minerals with a small proportion of calcite. Outlines of aligned tabular sericitized plagioclase feldspar can be seen, which are up 2 mm across. Patches of green epidote and oxides up to 1 mm across are present and there are small regions of squat, altered clinopyroxene. The rocks with obvious plagioclase crystals may be porphyritic basalts or basaltic andesites of an extrusive or hypabyssal nature.

Analytical methods

U–Pb zircon geochronology

A single fresh granitoid (317UPb) from dredge EA6811317 was selected for U–Pb zircon dating. Approximately 200 zircons were recovered using the Ammann AG selFrag machine and electromagnetic separation at the Technical University of Freiberg. selFrag applies a high-voltage pulse that disaggregates samples by introducing a short-lived plasma channel of 1–2 µm between grain boundaries (Gnos *et al.* 2006). Fifty zircon grains of 100–150 µm were selected and mounted in epoxy resin with chips of TEMORA (Middledale gabbro–diorite of New South Wales, Australia) and 91500 (geostandard) reference zircons. Grains were half-sectioned and polished. Reflected and transmitted light photomicrographs and cathodoluminescence images (CL) were prepared. The CL images were used to decipher internal structures and to identify target specific areas.

U–Pb analyses were carried out by sensitive high-resolution ion microprobe (SHRIMP) using a SHRIMP-II at the Center for Isotopic Research, VSEGEI, St. Petersburg, Russia. Twelve sites on eight zircons were selected. Each analysis consisted of five scans through the mass range, with spot diameter *c*. 25 µm and primary beam intensity *c*. 10 nA. The data have been reduced in a manner similar to that described by Williams (1998, and references therein) using the SQUID Excel Macro of Ludwig (2000). Pb/U ratios have been normalized relative to a value of 0.0668 for the $^{206}Pb/^{238}U$ ratio of the TEMORA reference zircons, equivalent to an age of 416.75 Ma (Black *et al.* 2003). Uncertainties for single analyses (ratios and ages) are at the 1σ level; however, uncertainties in calculated concordia ages are reported at the 2σ level. The inverse concordia plot (Fig. 2) has been prepared using ISOPLOT/EX (Ludwig 1999). Results are presented in Table 1.

Major and trace elements

Whole-rock samples were prepared and analysed for major and trace elements at Cardiff University in accordance with the fluxy-fusion method outlined by McDonald & Viljoen (2006) and Hastie *et al.* (2009). Loss-on-ignition (LOI) values were calculated following heating at 900 °C for 2 h. Ignited samples were fused and dissolved in dilute nitric acid. Major elements and Sc were analysed by inductively coupled plasma optical emission spectrometry (ICP-OES) on a JY Horiba Ultima 2. All other trace elements were analysed by inductively coupled plasma mass spectrometry (ICP-MS) (Thermo X7 series). Silicate rock standards JB-1a, NIM-G and BIR-1 were run through repeated sample batches. Relative standard deviations show precision of 1–5% for most major and trace elements; 2σ values encompass certified values for the vast majority of elements. Representative analyses are shown in Table 2.

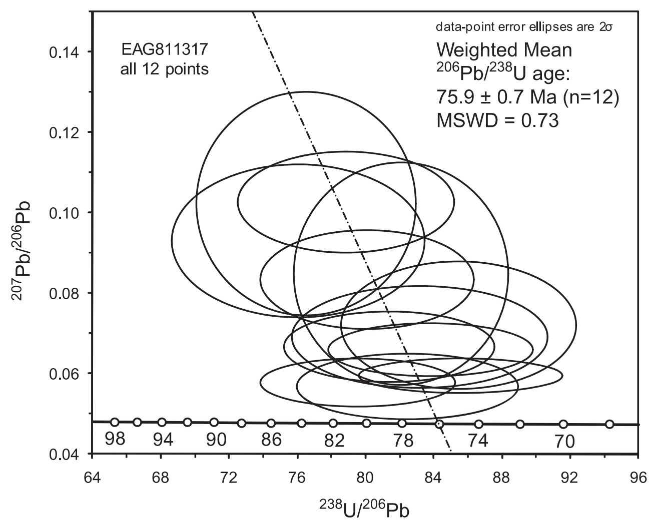

Fig. 2. Inverse concordia plot for zircon U–Pb analyses of granitoid sample 317UPb.

Table 1. *U–Pb zircon SHRIMP results for sample 317UPb*

Spot	^{206}Pb* (%)	U (ppm)	Th (ppm)	^{232}Th/^{238}U	^{206}Pb† (ppm)	Total ^{238}U/^{206}Pb	±%	Total ^{207}Pb/^{206}Pb	±%	^{206}Pb/^{238}U age‡ (Ma)
EA6811317UPb.1.1	3.86	64	21	0.33	0.724	76	4	0.093	8.3	79.4 ± 3.2
EA6811317UPb.2.1	15.63	84	30	0.37	0.877	82.5	3.2	0.0568	5.9	76.8 ± 2.5
EA6811317UPb.4.1	5.96	106	35	0.35	1.11	82.1	3.1	0.085	13	74.4 ± 2.6
EA6811317UPb.4.2	13.71	73	27	0.38	0.794	78.9	3.3	0.1026	5	75.6 ± 2.5
EA6811317UPb.3.1	7.37	119	47	0.41	1.23	83.2	3.7	0.0692	7.5	74.9 ± 2.8
EA6811317UPb.5.1	6.99	123	47	0.40	1.3	81.4	3.1	0.0667	5.3	76.8 ± 2.4
EA6811317UPb.5.2	2.81	427	287	0.69	4.28	85.6	2.8	0.0595	3	73.8 ± 2.1
EA6811317UPb.7.1	14.03	79	29	0.38	0.79	85.4	3.3	0.0721	9	72.7 ± 2.5
EA6811317UPb.7.2	29.44	56	15	0.27	0.629	76.5	3.4	0.102	11	77.9 ± 2.9
EA6811317UPb.6.1	20.28	200	120	0.62	2.05	83.8	2.9	0.0659	4.1	74.7 ± 2.2
EA6811317UPb.8.1	15.69	94	40	0.44	1	80.1	3.2	0.0835	6	76.4 ± 2.5
EA6811317UPb.8.2	10.71	197	80	0.42	2.13	79.5	2.9	0.0578	4.3	79.5 ± 2.3

Errors in the age calculation are at 1σ. Error in standard calibration was 0.90% (not included in above errors but required when comparing data from different mounts).
*Common Pb proportion.
†Radiogenic Pb proportion.
‡Common Pb corrected assuming ^{206}Pb/^{238}U–^{207}Pb/^{235}U age-concordance.

Nd and Hf radiogenic isotopes

Nd and Hf isotope compositions were analysed at the NERC Isotope Geoscience Laboratories, Nottingham, UK. Full analytical details have been given by Hastie *et al.* (2009) and results are presented in Table 3. For Hf isotope analysis, the samples were prepared following the procedures of Münker *et al.* (2001), and analysed by ICP-MS using a Nu-Plasma multicollector ICP-MS system. Hf blanks were less than 100 pg. Replicate analysis of the JMC475 standard gave ^{176}Hf/^{177}Hf = 0.282161 ± 0.000006 (1σ, $n = 45$), directly comparable with the preferred value of 0.282160 (Nowell & Parrish 2001). Replicate analysis of BCR-2 gave ^{176}Hf/^{177}Hf = 0.282866 ± 0.000006 (1σ, $n = 7$), similar to the previously reported value of 0.282879 ± 0.000008 (Blichert-Toft 2001). Determinations of Nd isotopes followed the procedures of Kempton (1995) and Royse *et al.* (1998). Nd was run as the metal species using double Re–Ta filaments on a Finnigan Triton mass spectrometer. Replicate analysis of the La Jolla standard gave a value of ^{143}Nd/^{144}Nd = 0.511846 ± 0.000003 (1σ, $n = 6$) and results are normalized to a preferred value of 0.511860.

Results

U–Pb zircon age

The zircons imaged by CL are generally clear, with magmatic zoning throughout, and lack rounded (inherited) cores. Many are prismatic, euhedral crystals. All 12 analyses from eight zircon grains yield a concordant age with no sign of discordance or inheritance on the ^{207}Pb/^{206}Pb v. ^{238}U/^{206}Pb inverse concordia plot (Fig. 2). Assuming ^{206}Pb/^{238}U–^{207}Pb/^{235}U age-concordance, the weighted mean of ^{206}Pb/^{238}U ages (Table 1) is 75.9 ± 0.7 Ma (mean square weighted deviation (MSWD) = 0.73), which we interpret as the crystallization age of the granitoid.

Alteration and elemental mobility

Many geochemical studies have shown that most major elements and large ion lithophile elements (LILE) are mobilized by sub-solidus processes such as hydrothermal alteration, metamorphism and weathering (e.g. Seewald & Seyfried 1990; Hastie *et al.* 2007). To test element mobility, elements are plotted against a known incompatible immobile element, in this case Nb (Fig. 3). Within a given magmatic suite, samples should form coherent liquid lines of descent. For the Aves Ridge samples the high field strength elements (HFSE) and the rare earth elements (REE) in the mafic rocks display good correlations with Nb. These correlations indicate that (1) these elements have been relatively immobile during sub-solidus alteration, despite LOI values of *c.* 3–15%, and so may be used to investigate the origin of the mafic rocks, and (2) the mafic rocks are part of one cogenetic suite. As the granitoids are evolved and fairly uniform in composition they do not show liquid lines of descent in Figure 3. Nevertheless, the granitoids can be investigated using the immobile HFSE and REE as, despite some epidotization, the rocks are relatively fresh and not silicified or calcified, with LOI values of *c.* 1%. The Mn-oxide coating on many granitoid samples may have acted as a protective layer.

Granitoid major and trace element geochemistry

SiO_2 spans a narrow range from 67 to 72 wt%. The granitoids have low abundances of TiO_2 (0.4 wt%), Fe_2O_3 (3.5 wt%) and MgO (<1.5 wt%). These rocks have elevated Ba (up to 1095 ppm) and Sr (up to 444 ppm) contents and low Cr (<24 ppm), V (*c.* 70 ppm), Co (<7.5 ppm) and Ni (<46 ppm). Compared with the mafic rocks, the granitoids have lower contents of Sm and Sc and higher abundances of Sr and Zr (Fig. 3). There is no clear magmatic differentiation trend between the most evolved mafic rocks and the least evolved felsic rocks for any immobile elements shown. Both granitic dredges show identical, slightly concave-up, chondrite-normalized (CN) REE patterns (Fig. 4). The samples are light REE (LREE) enriched with an average La/Yb_{CN} of 4.5 consistent with a calc-alkaline affinity and there is slight heavy/middle REE (HREE/MREE) enrichment. On an normal mid-ocean ridge basalt (N-MORB)-normalized (NMN) plot (Fig. 4) the granitoids are LREE/HREE enriched and have positive Zr–Hf and Th anomalies along with negative Nb–Ta and Ti anomalies.

Mafic rock major and trace element geochemistry

SiO_2 ranges from 34 to 57 wt%, MgO from 1 to 6 wt%, Al_2O_3 from 11 to 22 wt% and $Na_2O + K_2O$ from 3 to 11 wt%. TiO_2 has a much narrower range of concentrations than other major

Table 2. *Representative elemental data for the Aves Ridge*

Dredge:	317a	319d	318a	318b	318c	318d	318e	318g
Type:	CAA–G	CAA–G	IAT–BA	IAT–BA	CAA–BAS	CAA–BA	CAA–BA	CAA–BA
Major elements (wt%)								
SiO_2	68.13	70.64	43.41	44.99	49.75	52.88	49.32	54.02
TiO_2	0.43	0.40	0.63	0.59	0.74	0.68	0.79	0.68
Al_2O_3	15.23	13.50	20.49	22.43	16.79	13.98	17.06	14.73
$Fe_2O_3{}^T$	3.92	3.50	10.04	8.72	12.14	9.53	9.85	8.58
MnO	0.08	0.11	0.21	0.15	0.50	0.49	0.44	0.41
MgO	1.29	1.09	5.52	4.58	2.56	1.11	2.47	1.35
CaO	3.61	3.12	7.42	7.19	2.05	4.76	3.18	3.69
Na_2O	3.84	3.38	3.85	3.68	0.17	0.19	0.16	0.26
K_2O	2.35	2.72	1.28	1.44	10.14	10.09	10.06	10.56
P_2O_5	0.17	0.18	0.20	0.24	1.09	1.73	0.86	1.80
LOI	0.99	1.14	7.09	5.29	3.54	4.77	5.24	3.45
Total	100.05	99.79	100.12	99.30	99.47	100.19	99.43	99.54
Trace elements (ppm)								
Sc	9.9	9.0	22.4	21.9	36.5	33.6	41.2	33.0
V	78.0	67.4	251.4	200.0	359.6	303.1	385.8	288.3
Cr	9.9	11.7	8.6	12.5	94.4	58.5	68.2	71.4
Co	6.7	6.0	30.7	22.6	30.1	16.7	23.3	19.9
Ni	8.1	1.3	48.9	34.4	102.7	137.0	89.8	84.9
Cu	16.6	12.7	107.9	115.2	101.6	115.2	135.7	103.7
Ga	12.6	12.1	15.2	16.0	14.6	7.8	18.2	9.7
Rb	26.4	32.6	20.5	18.0	99.0	82.1	106.1	90.5
Sr	405	387	619	903	106	152	124	144
Y	19.8	18.2	13.6	14.1	34.4	25.5	33.7	25.4
Zr	127.2	138.2	29.5	31.8	64.7	58.5	74.9	52.0
Nb	4.13	4.78	1.16	1.12	4.75	3.78	5.08	3.99
Ba	698	772	230	424	6193	5699	5868	5930
Hf	2.94	3.24	0.76	0.83	1.62	1.39	1.83	1.17
Ta	0.29	0.36	0.07	0.07	0.33	0.28	0.36	0.29
Pb	3.21	3.22	3.47	1.80	30.07	30.80	13.95	20.53
Th	1.86	2.10	0.58	0.30	1.78	1.55	1.88	1.60
U	0.81	0.73	0.32	0.24	2.65	4.12	1.80	2.44
La	13.91	12.64	4.29	4.81	14.93	15.64	18.72	14.91
Ce	30.79	27.73	10.83	11.69	33.69	23.73	28.07	24.76
Pr	4.11	3.69	1.56	1.81	5.48	3.57	4.36	3.85
Nd	17.47	15.54	7.69	8.94	25.77	16.21	20.05	17.04
Sm	3.74	3.29	2.06	2.33	5.97	3.77	4.86	3.76
Eu	1.05	0.96	0.72	0.83	2.93	1.43	1.71	1.51
Gd	3.31	2.93	2.07	2.33	5.76	3.63	4.77	3.60
Tb	0.48	0.44	0.33	0.36	0.76	0.54	0.72	0.52
Dy	2.97	2.74	2.17	2.32	4.33	3.44	4.62	3.28
Ho	0.59	0.55	0.43	0.45	0.80	0.69	0.94	0.67
Er	1.80	1.69	1.28	1.32	2.20	2.07	2.84	1.97
Tm	0.31	0.28	0.20	0.21	0.33	0.32	0.45	0.31
Yb	2.04	1.97	1.36	1.39	2.06	2.06	2.91	1.95
Lu	0.34	0.34	0.22	0.22	0.32	0.34	0.47	0.32

All dredges prefixed EA68-11. LOI, loss on ignition; CAA, calc-alkaline arc; IAT, island arc tholeiite; G, granite; BA, basaltic andesite; BAS, basalt.

Table 3. *Nd–Hf radiogenic isotope data from the Aves Ridge*

Sample	$^{147}Sm/^{144}Nd$	$^{143}Nd/^{144}Nd$	$^{143}Nd/^{144}Nd(i)$	εNd(i)	$^{176}Lu/^{177}Hf$	$^{176}Hf/^{177}Hf$	$^{176}Hf/^{177}Hf(i)$	εHf(i)
EA68 11317a	0.1333662	0.513000	0.512934	7.677	0.0164336	0.283178	0.283154	15.185
EA68 11318g	0.1293869	0.512843	0.512779	4.653	0.0388652	0.283112	0.283057	11.756

(i), values are age corrected to 76 Ma.

elements, from 0.5 to 0.8 wt%. When plotted against Nb, MgO and Al_2O_3 show a weak positive correlation (Fig. 3). As these samples are altered, classification based on major elements is impractical, so we use the Th–Co plot of Hastie *et al.* (2007) (Fig. 5). This diagram, based on a global arc dataset, uses Th and Co as immobile proxies for the SiO_2–K_2O discrimination diagram of Peccarillo & Taylor (1976). Figure 5 shows that the rocks mostly classify as basaltic andesites of calc-alkaline affinity, although two samples plot in the tholeiite field.

The mafic samples have LREE-enriched chondrite-normalized REE patterns (Fig. 4). Nine samples have La/Yb_{CN} ratios of about five (calc-alkaline), whereas two are less LREE-enriched and have La/Yb_{CN} values of about two (tholeiitic), in line with the Th–Co diagram (Fig. 5). The most enriched calc-alkaline

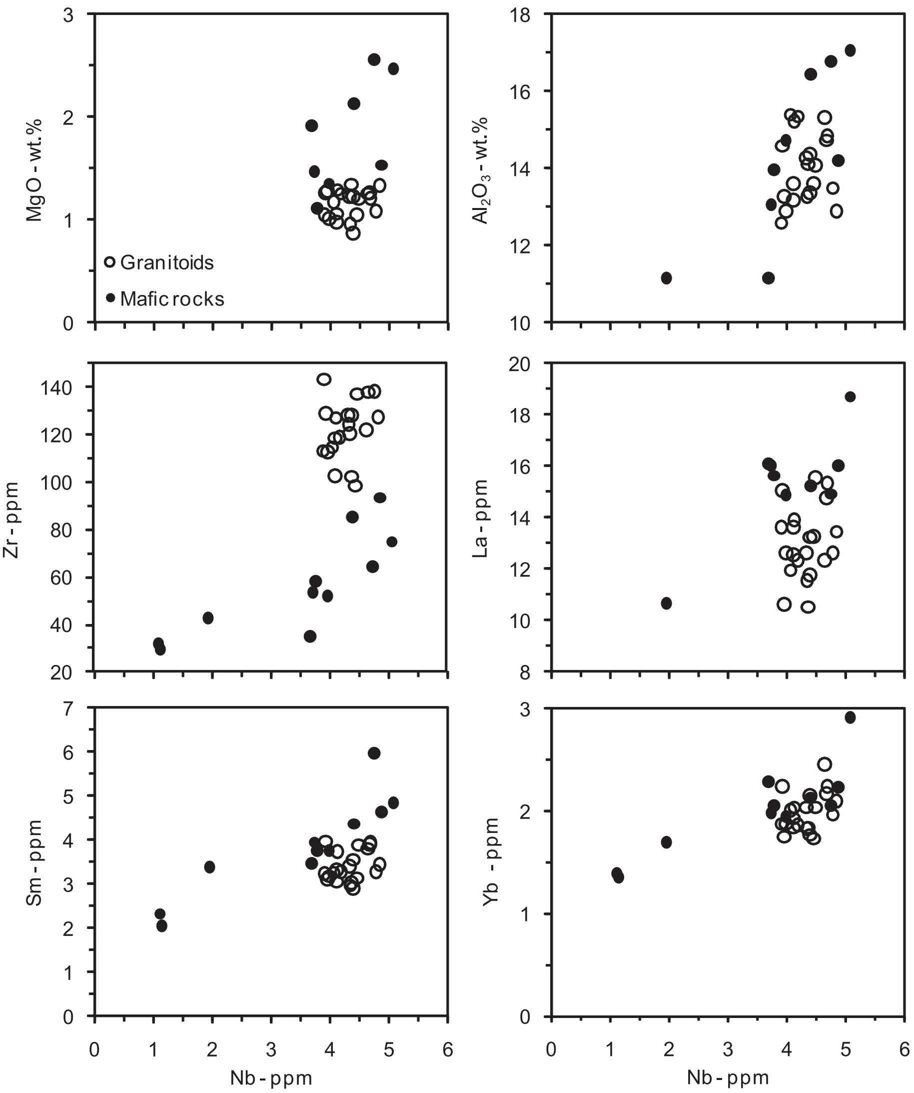

Fig. 3. Variation diagrams for selected elements for both granitoids and mafic rocks.

samples show a small positive Eu anomaly. The HREE and MREE in these mafic rocks are not depleted relative to N-MORB (Fig. 4). Negative Ce anomalies are also present in some of the mafic samples, which do not correlate with LOI values and are therefore unlikely to be related to sub-solidus alteration processes. On the N-MORB-normalized trace element plot (Fig. 4), all samples show significant Th enrichment and Nb–Ta and Ti depletions (e.g. $Nb/La_{NMN} = 0.20–0.33$). In contrast to the granitoid rocks, the mafic samples have negative Zr–Hf anomalies.

Nd and Hf radiogenic isotopes

Radiogenic Nd and Hf isotope data for granitoid and basaltic andesite samples are shown in Table 3 and Figure 6. The results have been age-corrected to 76 Ma and are markedly distinct from one another. The granitoid sample has a relatively depleted signature ($\varepsilon_{Ndi} = +7.68$ and $\varepsilon_{Hfi} = +15.19$), whereas the basaltic andesite is less depleted with $\varepsilon_{Ndi} = +4.65$ and $\varepsilon_{Hfi} = +11.76$. The granitoid plots well within the main Caribbean–Colombian Oceanic Plateau field (Hastie *et al.* 2009) on the ε_{Hfi} v. ε_{Ndi} diagram, but the basaltic andesite has a more enriched isotopic signature similar to the present-day Lesser Antilles arc (White & Patchett 1984). Both samples have higher ε_{Hfi} than Pacific MORB. The field for present-day Pacific MORB has not been age-corrected, as Thompson *et al.* (2003) demonstrated that present-day and Jurassic Pacific MORB were isotopically very similar and predicted that the Hf isotope composition within a uniform chondritic reservoir would change by <0.5 epsilon units in 90 Ma.

Discussion

Are the granitoids and mafic rocks cogenetic?

The variation diagrams (Fig. 3) show that the mafic rocks define, in the case of the immobile and incompatible elements, clear intra-magmatic differentiation trends, which may be related to crystal fractionation. The granitoid rocks plot in a distinct field at lower incompatible element concentrations than the most evolved mafic rocks with the exception of Zr, and display no coherent liquid line of descent compatible with the mafic rocks. This shows that the mafic and felsic rocks are not related to each other by fractional crystallization processes. The negative Zr–Hf

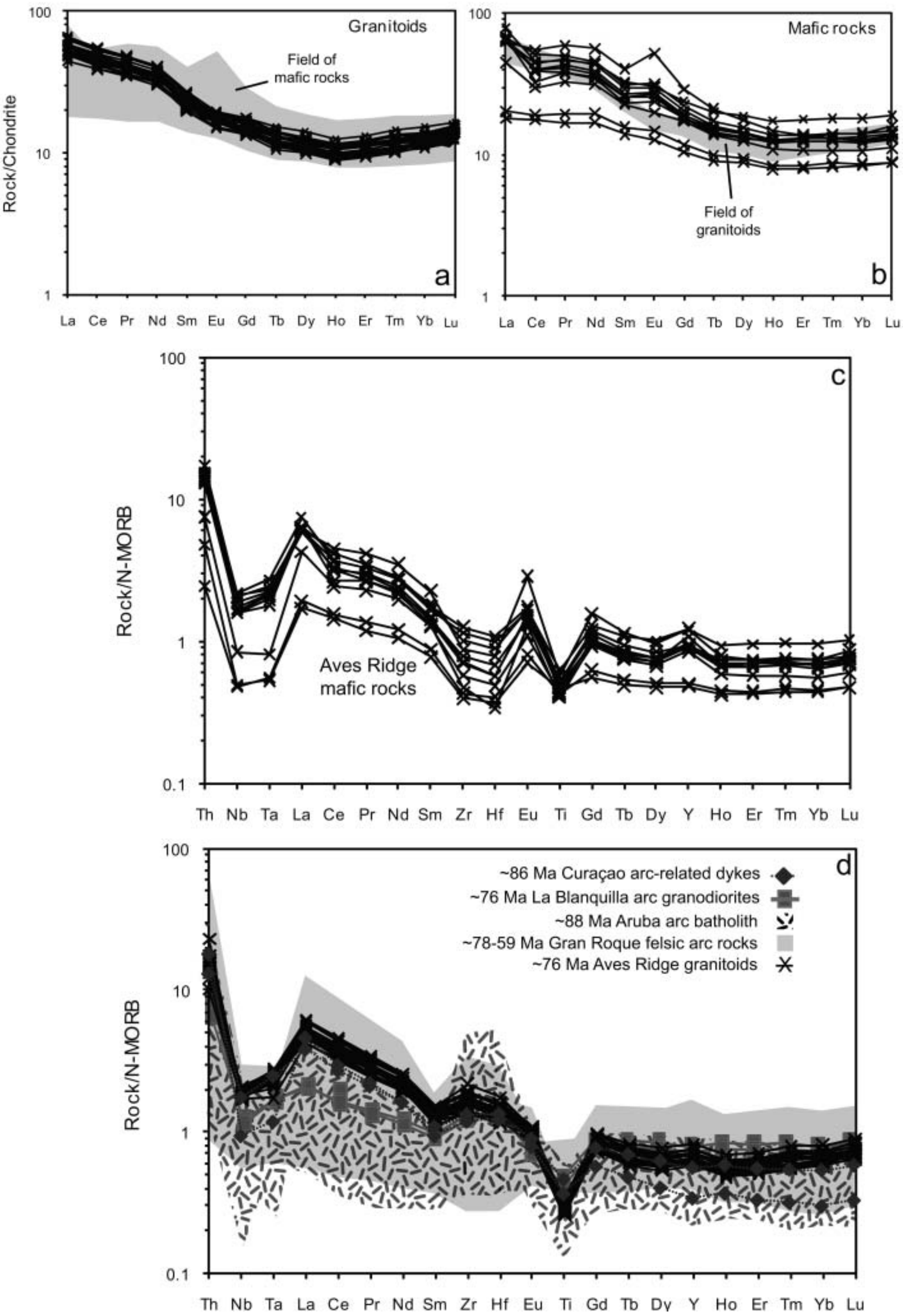

Fig. 4. Chondrite-normalized REE plots for: (**a**) Aves Ridge granitoids and (**b**) mafic rocks using normalizing values from Sun & McDonough (1989). Multi-element plots for (**c**) for the Aves Ridge mafic rocks and (**d**) the Aves Ridge granitoids compared with Gran Roque arc granodiorites (Wright & Wyld 2010; A. C. Kerr, unpublished data), Aruba batholith (White *et al.* 1999) and Curaçao–La Blanquilla arc intrusions (Wright & Wyld 2010). N-MORB-normalizing values from McDonough & Sun (1995).

anomalies on the multi-element plot for the mafic rocks (Fig. 4c), indicated by Zr/Sm_{NMN} <1, are likely to be related to subduction-related REE enrichment (Thirlwall *et al.* 1994). On the other hand, the positive Zr–Hf anomalies for the granitoids (Fig. 4d) may indicate that these rocks have accumulated zircon, or that their source contained residual amphibole, because amphibole is more compatible with the MREE than Zr or Hf (Klein *et al.* 1997). These different Zr–Hf anomalies again point to distinct origins for the mafic and granitoid rocks. Most importantly, crystal fractionation cannot explain the different ε_{Ndi} and ε_{Hfi} isotopic ratios in Figure 6, so although only two analyses are available it is concluded that the mafic and granitoid rocks of the Aves Ridge are not derived from the same source region. However, without field relationships with which to test the relative age of the mafic and felsic samples and without dateable mafic material, the age of the mafic rocks in this study remains uncertain.

Island arc origin of the southeastern Aves Ridge

The presence of negative Nb–Ta anomalies on N-MORB-normalized plots (Fig. 4) is usually regarded as indicative of subduction zone processes, as Nb and Ta are preferentially held in rutile in the downgoing slab during aqueous fluid release (e.g. Saunders *et al.* 1980; Thirlwall *et al.* 1994). Furthermore, the Th/Yb v. Ta/Yb diagram of Pearce (1983) (Fig. 7a) shows that the mafic rocks plot above the MORB array, which suggests that they have a subduction zone affinity. The radiogenic isotope

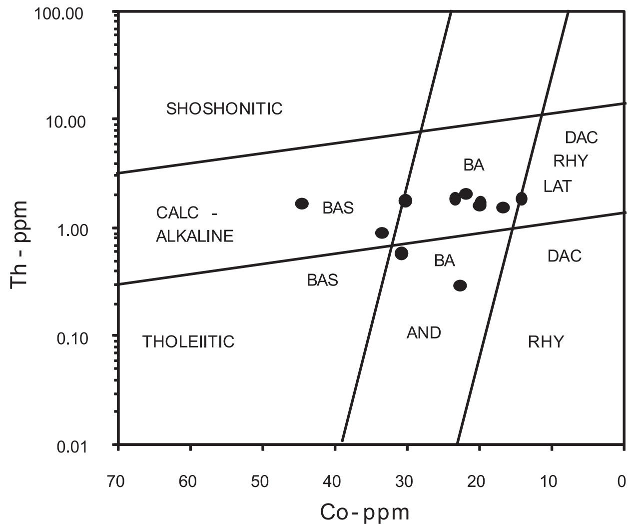

Fig. 5. Th–Co diagram (Hastie *et al.* 2007) for the Aves Ridge mafic rocks. BAS, basalt; BA, basaltic andesite; AND, andesite; DAC, dacite; RHY, rhyolite; LAT, latite.

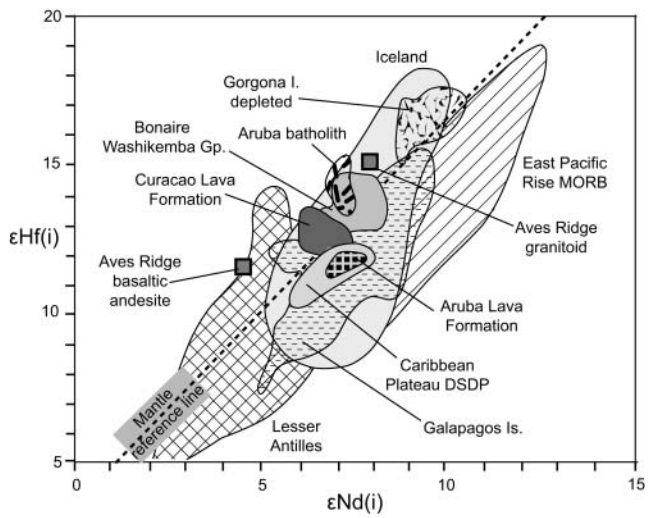

Fig. 6. Hf–Nd radiogenic isotope plot for the Aves Ridge rocks. Fields from Thompson *et al.* (2003, 2004) apart from the Lesser Antilles (White & Patchett 1984).

ratios of the mafic and granitoid rocks (Fig. 6) and zircons without rounded, inherited cores from the granitoids do not indicate contamination from old continental crustal material, an alternative source of negative Nb–Ta anomalies. Therefore, geochemical evidence, confirmed by existing geophysical and geodynamic models, shows that the Aves Ridge represents the eroded products of an extinct subduction zone.

Source of the granitoid rocks

As the granitoids were sampled from only two outcrops, their lack of geochemical variation may be indicative of a sampling bias rather than a distinct petrogenetic feature. However, some petrological and geochemical constraints can be used to discuss their source region.

We rule out the possibility that the granitoids formed by partial melting of a subducting oceanic slab, to generate an acidic melt (e.g. Drummond & Defant 1990). Such a melt could interact with the mantle wedge beneath the Aves Ridge arc, and generate higher MgO, Ni and Cr concentrations and lower SiO_2 contents in a subsequent melt (high-Mg andesite) (e.g. Rapp *et al.* 1999). However, as noted, the granitoids have very low concentrations of mantle-derived elements and are siliceous (SiO_2 *c.* 70 wt%). Slab fusion during subduction occurs only in anomalously hot subduction zones and largely at depths where residual garnet would cause HREE depletion in the resulting felsic melts, a feature also not seen in the granitoids (Drummond & Defant 1990; Peacock *et al.* 1994; Drummond *et al.* 1996; Rapp *et al.* 2003). We also argue that the granitoids did not form by fractional crystallization from a mafic, mantle-derived melt because the mafic and granitoid rocks are not cogenetic.

Our preferred hypothesis is that the granitoids are of crustal origin. In this model, the fine-grained hornblende-rich intermediate facies present within the granitoids are interpreted to be I-type restite and the granitoids are considered to have been formed by the partial melting of the mafic lower crust (Chappell *et al.* 1987; Drummond *et al.* 1996; Stephens 2001). Additionally, SiO_2 concentrations of 67–72 wt% and a sodic character ($Na_2O/K_2O = 1.65$) are compatible with re-melting of a tholeiitic mafic source at moderate (10–20%) degrees of partial melting (Rapp & Watson 1995). The positive Zr–Hf anomalies (see above) and moderate Sr concentrations (up to 440 ppm) suggest that amphibole and plagioclase may have remained in the source residue of the granitoids. Moderate levels of Y (>16 ppm) and the HREE (Yb >1.7 ppm) and low La/Yb (*c.* 6.6) rule out residual garnet and constrain partial melting to <30 km depth (see Drummond & Defant 1990; Rapp & Watson 1995). If the granitoids are derived from a mafic protolith, their negative Nb–Ta anomalies (Fig. 4) might be attributed to re-melting of the lower Aves Ridge arc crust by advection owing to the underplating of hot basaltic arc magma (Petford *et al.* 2000; Petford & Gallacher 2001).

Source of the mafic rocks: mantle wedge component

Unlike the granitoids, the mafic rocks have high concentrations of Mg, Ni and Cr indicating derivation from a peridotitic mantle source beneath the Aves Ridge. As the MREE and HREE are not depleted on the normalized plots (Fig. 4), garnet was not present in the source or was completely melted out during partial melting. In the former case, the depth of partial melting is constrained to above the approximate spinel–garnet transition at <55 km within the mantle (Su, 2008).

Of particular interest is the composition of the mantle wedge source, but any investigation must first assess whether the wedge was fluxed by slab- and sediment-related fluids alone, or also by slab-derived partial melts. The HFSE and HREE are normally used to investigate the composition of the mantle wedge, but these elements can be mobilized from the slab if it partially melts (Pearce & Peate 1995). Figure 7b (Zr/Yb v. Nb/Yb) shows that the mafic samples plot within the MORB array, suggesting that the HFSE and HREE have not been mobilized from the slab to the wedge. Therefore, variations in the HFSE and HREE can be explained by partial melting and fractional crystallization processes and the composition of the mantle wedge. We focus on Zr and Nb in particular because in mafic rocks, Zr and Nb behave

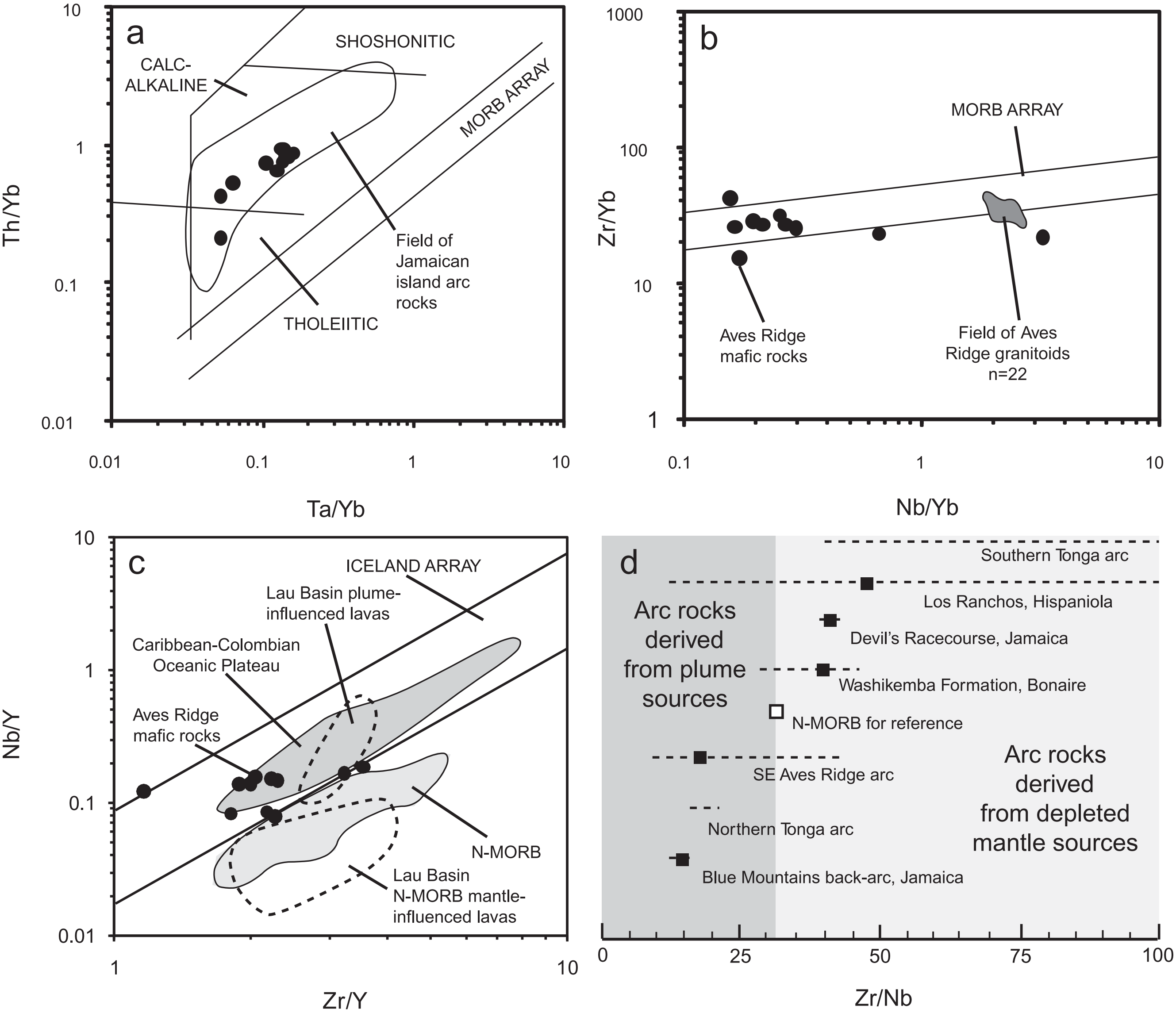

Fig. 7. Trace element ratio plots: (**a**) Th/Yb v. Ta/Yb plot (Pearce 1983) showing the Aves Ridge mafic rocks compared with arc rocks from Jamaica (Hastie *et al.* 2009); (**b**) Zr/Yb v. Nb/Yb plot (Pearce & Peate 1995) for the mafic and granitoid rocks of the Aves Ridge; (**c**) Nb/Y v. Zr/Y diagram (Fitton *et al.* 1997) for the mafic rocks of the Aves Ridge showing the Caribbean–Colombian Oceanic Plateau field of Hastie *et al.* (2008), N-MORB from Fitton *et al.* (1997) and the Lau Basin from Hastie *et al.* (2010); (**d**) Zr/Nb ratios with mean values (squares) and ranges (dotted lines) for selected mafic arc and oceanic plateau occurrences in the Caribbean region and Tonga arc. Sources: Blue Mountains back-arc basin, Jamaica, Hastie *et al.* (2010); Curacao Lava Formation, Kerr *et al.* (1996) and Hauff *et al.* (2000); Devil's Racecourse Formation, Jamaica, Hastie *et al.* (2009); Los Ranchos Formation, Hispaniola, Escuder Viruete *et al.* (2006); N-MORB, Sun & McDonough (1989); Tongan arc, Wendt *et al.* (1997); Washikemba Group, Bonaire, Thompson *et al.* (2004).

similarly during fractional crystallization of the major phases. Additionally, Zr and Nb behave incompatibly between the main mineral species of mantle peridotite and a coexisting partial melt (e.g. Salters *et al.* 2002). Therefore, unless the partial melt volume is extremely small, the Zr/Nb ratio will not vary significantly with the degree of partial melting. Island arc magmas are generated by 15–30% partial melting (Pearce & Parkinson 1993; Pearce & Stern 2006), therefore the Zr/Nb ratio of the mafic rocks of the Aves Ridge should represent the composition of the source region.

The Nb/Y v. Zr/Y plot (Fig. 7c) distinguishes mafic rocks derived from depleted MORB mantle (DMM) and mantle plume sources that are enriched in Nb relative to MORB (Fitton *et al.* 1997). The plot has been used to identify Caribbean–Colombian Oceanic Plateau lavas (e.g. Kerr *et al.* 2009), and to discriminate between island arc rocks derived from depleted mantle wedges and those derived from plume-enriched sources in the Caribbean region (Hastie *et al.* 2010; Neill *et al.* 2010). High Nb/Y in relation to N-MORB-like rocks may indicate a plume mantle wedge source, as shown by Hastie *et al.* (2010) for the Lau Basin. The Aves Ridge rocks plot within and around the 'Iceland array', along with the plume-influenced Lau Basin lavas (Fig. 7c), consistent with the idea that the mantle wedge beneath the Aves Ridge may have been of mantle plume composition.

In average N-MORB, Zr/Nb is *c*. 32 (Sun & McDonough

1989) but in mafic arc rocks, Zr/Nb ratios range from *c*. 40 to 120 (Wendt *et al.* 1997). It is difficult, except at unrealistically low degrees of partial melting, to produce Zr/Nb <32 during partial melting of DMM. Therefore, Zr/Nb <32 in arc rocks may indicate a plume-related mantle wedge as shown for lavas erupted in the Tongan arc and in Jamaica (Wendt *et al.* 1997; Hastie *et al.* 2010). Rocks from the southern Tongan arc are derived from a depleted source and have Zr/Nb ratios >40, whereas those from the Samoan plume-influenced northern Tonga region have Zr/Nb ratios of 16–21 (Wendt *et al.* 1997; Fig. 7d). Zr/Nb ratios for the Caribbean region are also shown in Figure 7d. Many pre-Caribbean–Colombian Oceanic Plateau Caribbean island arc lavas such as those on Bonaire (Thompson *et al.* 2004), Hispaniola (Escuder Viruete *et al.* 2006) and Jamaica (Hastie 2009), show high Zr/Nb ratios (>40) consistent with derivation from DMM. In contrast, the Aves Ridge rocks have Zr/Nb = 9–38 (mean = 17.7), much closer to the values for the plume-influenced *c*. 72 Ma Blue Mountains back-arc lavas in Jamaica (Hastie *et al.* 2010) and northern Tonga (Wendt *et al.* 1997). It is therefore likely that the low Zr/Nb ratios of the Aves Ridge mafic rocks have been derived from partial melting of a mantle wedge composed of mantle plume material.

Source of the mafic rocks: slab-flux component

Th and La are widely regarded to be mobilized from the slab by aqueous fluids during dehydration reactions in a subducting plate (Plank 2005; Hastie *et al.* 2007). Terrigenous sediments and the continental crust have high Th/La ratios of >0.2 whereas DMM and mantle plume sources range from 0.048 to 0.11 (Plank 2005). Accordingly, many island and continental arc rocks typically range from low mantle-like Th/La to high terrigenous sediment-like Th/La ratios (Plank 2005) depending on the volume of terrigenous sediment subducted. The Aves Ridge mafic rocks have consistently low Th/La ratios (<0.13), which indicate that there was little subducted terrigenous sediment in their source region.

In oxidizing pelagic sediment and red clay, Ce^{3+} is oxidized to Ce^{4+}, which is more soluble than La^{3+} in aqueous slab-derived fluids, thus leading to Ce depletion (Ce/Ce* <1) in the resultant island arc magmas (Hole *et al.* 1984). Ce/Ce* is the ratio of observed to expected Ce concentration on an N-MORB-normalized REE plot, with $Ce^* = ((La - Pr)/2) + Pr$. The Th/La v. Ce/Ce* diagram (Fig. 8) discriminates between terrigenous and pelagic sedimentary sources in arc rocks (Hastie *et al.* 2009; Neill *et al.* 2010). The mafic rocks from the Aves Ridge show a clear trend from mantle-like Ce/Ce* values of *c*. 1.0–0.58, indicating a significant involvement of pelagic sediment in the source region. The mafic rocks of the Aves Ridge therefore most probably formed in an intra-oceanic setting away from terrigenous proto-Caribbean passive margin sedimentary sequences or continental masses.

Correlation with the Dutch–Venezuelan Antilles

The age and origin of the recently studied rocks of the Dutch–Venezuelan Antilles are summarized in Table 4. In the Venezuelan Antilles, La Blanquilla contains the closest exposure of igneous rocks to the Aves Ridge (Fig. 1), where granodiorites and tonalites dated at *c*. 76 and *c*. 59 Ma respectively are found (Wright & Wyld 2010). The granodiorite is geochemically comparable with the Aves Ridge granitoids (Fid. 4d), with similar Th/La, La/Yb and Nb/Yb ratios. Like the Aves Ridge, no Caribbean–Colombian Oceanic Plateau mafic rocks are found on La Blanquilla. However, on Gran Roque of the Los Roques

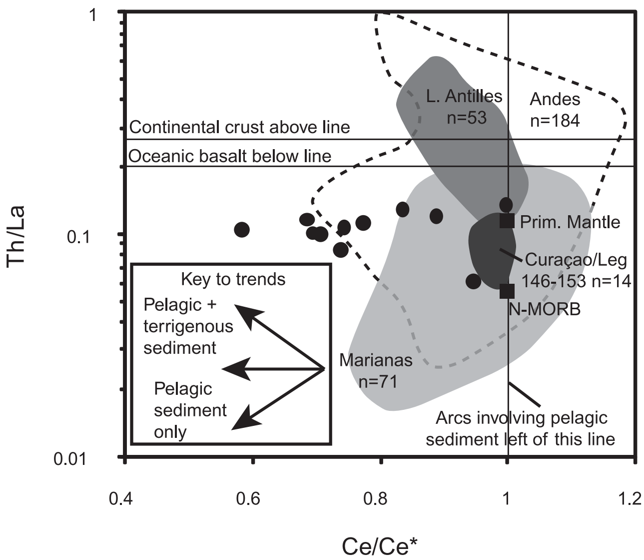

Fig. 8. Th/La v. Ce/Ce* plot for mafic arc rocks (Hastie *et al.* 2009). The Aves Ridge arc (filled circles) and the Marianas arc both subducted oxidized pelagic sediments. The Lesser Antilles and Andean arcs contain a subducted terrigenous sedimentary component. Marianas, Andean and Lesser Antilles arcs data are from the GEOROC database, available at http://georoc.mpch-mainz.gwdg.de/georoc (2009). Data for primitive mantle data from Sun & McDonough (1989), N-MORB from McDonough & Sun (1995), Curaçao from Hauff *et al.* (2000).

islands (Fig. 1), undated gabbros and dolerites of Caribbean–Colombian Oceanic Plateau affinity are present (Giunta *et al.* 2002; A. C. Kerr, unpublished data). The mafic rocks are cut by quartz diorites, pegmatites and aplites with Ar–Ar biotite and hornblende ages of *c*. 68 and *c*. 59 Ma respectively (van der Lelij *et al.* 2010). Like La Blanquilla, the felsic rocks of Los Roques have almost identical trace element signatures to the granitoids of the Aves Ridge (Fig. 4d; data from Giunta *et al.* 2002; A. C. Kerr, unpublished data). All the Venezuelan Antilles arc rocks are considered to be formed by NW- or west-dipping subduction beneath the Caribbean–Colombian Oceanic Plateau (Wright & Wyld 2010).

On Curaçao in the Dutch Antilles (Fig. 1), dykes of diorite and quartz diorite (*c*. 86 Ma; Wright & Wyld 2010) intrude the Caribbean–Colombian Oceanic Plateau-related Curaçao Lava Formation (*c*. 89 Ma; Sinton *et al.* 1998). These dykes also have very similar trace element signatures to the Aves Ridge granitoids (Fig. 4d; Wright & Wyld 2010). Aruba, also part of the Dutch Antilles (Fig. 1), includes the mafic Aruba Lava Formation, which is dated using the imprint of ammonite fossils to *c*. 90 Ma, and is a part of the Caribbean–Colombian Oceanic Plateau (MacDonald 1968; White *et al.* 1999). The Lava Formation is cut by the dioritic to tonalitic Aruba Batholith, which has a weighted mean U–Pb zircon age of 88.6 ± 0.5 Ma (van der Lelij *et al.* 2010; Wright & Wyld 2010). White *et al.* (1999) showed that the batholith has low Nb, high Ba and Sr, and flat to LREE-enriched REE patterns (Fig. 4d). Although much more variable in major and trace element concentration, the Aruba batholith does resemble the Aves Ridge granitoids and is considered, like the Curaçao dykes, to have formed by partial melting of Caribbean–Colombian Oceanic Plateau crust during west-dipping subduction (White *et al.*, 1999; van der Lelij *et al.* 2010; Wright & Wyld 2010).

Table 4. *Summary of recent studies of igneous exposures from the Aves Ridge, Dutch–Venezuelan Antilles*

Location	Suite	Rock types	Age(s) (Ma)*	Tectonic setting	References
SE Aves Ridge	n.a.	Felsic intrusive	76 ± 1.4	Island arc	This paper
	n.a.	Mafic extrusive and intrusive	n.a.	Island arc (plume mantle source)	This paper
La Blanquilla (Venezuelan Antilles)	n.a.	Felsic intrusive	75.5 ± 0.9	Island arc	Wright & Wyld (2010)
	n.a.	Felsic intrusive	58.7 ± 0.5	Island arc	Wright & Wyld (2010)
Gran Roque (Venezuelan Antilles)	n.a.	Mafic intrusive	n.a.	Oceanic plateau	Giunta *et al.* (2002), A. C. Kerr (unpublished data)
	n.a.	Felsic intrusive	65.3 ± 1.4, 68.30 ± 0.76, 58.93 ± 1.22	Island arc	van der Lelij *et al.* (2010), Wright & Wyld (2010)
Curaçao (Dutch Antilles)	Lava Fm.	Mafic extrusive	88.9 ± 0.8	Oceanic plateau	Sinton *et al.* (1998)
	n.a.	Intermediate intrusive	86.2 ± 1.1	Island arc	Wright & Wyld (2010)
Aruba (Dutch Antilles)	Lava Fm.	Mafic extrusive	Turonian (*c.* 90 Ma)†	Oceanic plateau	MacDonald (1968), White *et al.* (1999)
	Batholith	Mafic to felsic intrusive	88.6 ± 0.5‡	Island arc (plume mantle source)	White *et al.* (1999), van der Lelij *et al.* (2010), Wright & Wyld (2010)
Bonaire (Dutch Antilles)	Washikemba Group	Felsic extrusive, mafic intrusive	94.6 ± 1.4, 98.2 ± 0.6	Island arc (depleted mantle source)	Thompson *et al.* (2004) Wright & Wyld (2010)
	Matijs Group	Mafic intrusive	Albian (*c.* 112 Ma)§	Island arc	Wright & Wyld (2010)

*Unmarked samples dated by U–Pb or Ar–Ar methods (see original references).
†Sample dated using ammonite imprints.
‡Weighted mean of available ages.

The only other mafic island arc rocks in the Dutch–Venezuelan Antilles are found on Bonaire Island (Table 4; Fig. 1), which has two suites of Cretaceous igneous rocks (Thompson *et al.* 2004; Wright & Wyld, 2010). Poorly studied mafic stocks of the Matijs Group intruded Aptian or older argillites before deposition of a Coniacian conglomerate unit. The felsic volcanic rocks, diorites and dacites of the Washikemba Group (Washikemba Formation of Thompson *et al.* 2004) have an age of *c.* 96 Ma (Thompson *et al.* 2004; Wright & Wyld, 2010). These rocks were formed by subduction beneath a depleted mantle source (Fig. 7d; Thompson *et al.* 2004). There are no rocks of Caribbean–Colombian Oceanic Plateau affinity or rocks derived from a plume-related mantle source on Bonaire.

These results have profound implications for the tectonic evolution of the southern Caribbean (van der Lelij *et al.* 2010; Wright & Wyld 2010). Because the Caribbean–Colombian Oceanic Plateau rocks exposed on Aruba, Curaçao and Gran Roque show no sign of interaction with slab fluids (see the Curaçao field in Fig. 8), Hastie & Kerr (2010) stated that there must have been no active subduction zone beneath this part of the Caribbean–Colombian Oceanic Plateau during its formation. Therefore, the *c.* 96 Ma island arc rocks on Bonaire would represent east-dipping subduction in the region (van der Lelij *et al.* 2010), as a west-dipping subduction would result in contamination of the Caribbean–Colombian Oceanic Plateau mantle source with slab-related fluids. Wright & Wyld (2010) suggested that Bonaire is a slice of the Greater Antilles arc that moved into the southern Caribbean along strike-slip faults before the inception of the Aves Ridge, but because Bonaire is an integral part of the Dutch Antilles we prefer the interpretation of van der Lelij *et al.* (2010).

Following eruption of the Caribbean–Colombian Oceanic Plateau, subduction-related rocks formed on Aruba and Curaçao within only 1–3 Ma of plateau formation (Wright & Wyld 2010). Studies of andesitic volcanoes using the U–Th decay series have shown that subduction-related fluids are generated and added to the mantle wedge only a few hundred thousand years before eruption (e.g. Turner *et al.* 2000). Partial melting to form the Aruba batholith and Curaçao dykes could therefore have occurred above a subduction zone that initiated along the edge of the Caribbean–Colombian Oceanic Plateau almost immediately following its formation (see Niu *et al.* 2003; Wright & Wyld 2010), or by collision of the Caribbean–Colombian Oceanic Plateau with an east-dipping subduction zone, triggering a rapid polarity reversal at *c.* 89 Ma (van der Lelij *et al.* 2010).

There are no arc rocks younger than *c.* 88 Ma in the Dutch Antilles. van der Lelij *et al.* (2010) used fission-track dating to show that significant uplift occurred on Bonaire at *c.* 85–80 Ma, and the Campanian and younger Soebi Blanco Formation on Bonaire and the Knip Group and Midden Curaçao Formation of Curacao contain continental detritus (Priem *et al.* 1986; Wright & Wyld 2010). Subduction was probably terminated abruptly by collision of the South American margin with the incipient arc.

The comparison above shows that the Aves Ridge rocks formed contemporaneously with magmatism on Gran Roque and La Blanquilla. On La Blanquilla there is no Caribbean–Colombian Oceanic Plateau basement through which the arc rocks intruded, as may be the case for the Aves Ridge (see below). Therefore La Blanquilla appears to be a southern extension of the Aves Ridge. There are no rocks found on the small proportion of the Aves Ridge that has been studied, nor in the Venezuelan Antilles older or younger than *c.* 76 Ma and *c.* 59 Ma, respectively. It is possible that following cessation of magmatism in the Dutch Antilles, subduction transferred eastwards to the Venezuelan Antilles and Aves Ridge, before stalling with inception of the Grenada Basin.

Petrogenesis of the Aves Ridge and La Blanquilla Island

The results presented above are consistent with a model in which the Aves Ridge and La Blanquilla were generated during west-dipping subduction beneath the Caribbean–Colombian Oceanic Plateau between *c.* 76 and *c.* 59 Ma. However, it appears that neither location is in immediate contact with the Caribbean–

Colombian Oceanic Plateau. Much of the Venezuelan Basin has up to 20 km thick plateau crust but in the far SE corner of the basin, a region of some 40 000 km^2, the crustal thickness, minus sedimentary cover, is <5 km (Fig. 1; Diebold *et al.* 1981). This thin crust is considered to predate the Caribbean–Colombian Oceanic Plateau, based on seismic interpretation (Diebold *et al.* 1981; Mauffret & Leroy 1997), although drilling has never been undertaken in this part of the Caribbean Sea. If this thin crust turns out not to be oceanic plateau material, then it is unlikely that the southern Aves Ridge was generated by west-dipping subduction of the proto-Caribbean slab directly beneath the Caribbean–Colombian Oceanic Plateau. Therefore, mantle convection is likely to have brought plume mantle into the wedge above the Aves Ridge subduction zone. Also, we cannot rule out the possibility that there were pre-existing plateau or island arc fragments beneath the site of the Aves Ridge. Some workers have argued that the Caribbean–Colombian Oceanic Plateau dates back to *c*. 115 Ma (Mauffret & Leroy 1997) and in addition there are *c*. 90 Ma volcanic rocks with oceanic plateau-like chemistry cutting proto-Caribbean passive margin sediments at San Souci, Trinidad (Wadge & Macdonald 1985; I. Neill, unpublished data).

Our petrogenetic model (Fig. 9) therefore shows the Aves Ridge arc overlying a plume-related mantle wedge and a subducting proto-Caribbean slab. The slab fluids ascend into the mantle wedge and promote partial melting to generate the Aves mafic lavas. The granitoids form by partial melting of tholeiitic amphibole- and plagioclase-bearing rocks in the lower crust beneath the Aves Ridge arc. As mentioned above, it is possible that partial melting was aided by the rise of hot mafic island arc magmas, perhaps even those that formed the mafic rocks in this study.

It is unclear whether or not the crustal thickness of the Aves Ridge could be generated during a short *c*. 20 Ma post-Caribbean–Colombian Oceanic Plateau subduction history (see below) with a starting crustal thickness of only 5 km, the same as the thin crust of the SE Venezuelan Basin. Subduction rates, roll-back, sediment flux, slab dip and magma production vary from arc to arc, hence it is difficult to quantify how quickly arc crust may be generated. The Lesser Antilles, which has a *c*. 55 Ma history of *c*. 2 cm a^{-1} subduction, a similar rate to the Aves Ridge (Pindell & Kennan 2009) has built up 30–35 km of crust (Christeson *et al.* 2008). It is possible that the 26 km thick Aves crust was generated during its post-Caribbean–Colombian Oceanic Plateau history, but we repeat that the pre-existence of plateau-like crust or older island arc rocks should not be ruled out. It may be significant that the isotopic composition of the granitoid sample (Fig. 6) falls within the Caribbean–Colombian Oceanic Plateau field and that this sample is isotopically dissimilar to N-MORB or island arc rocks.

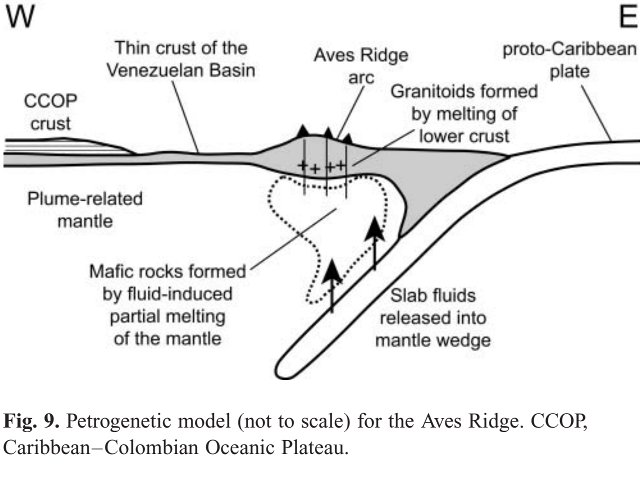

Fig. 9. Petrogenetic model (not to scale) for the Aves Ridge. CCOP, Caribbean–Colombian Oceanic Plateau.

Southern Caribbean tectonic model

In Figure 10, we outline a revised plate-tectonic model for the southern Caribbean based on the findings from the Aves Ridge and a new consideration of the origins of the Dutch–Venezuelan Antilles (van der Lelij *et al.* 2010; Wright & Wyld 2010). At *c*. 100 Ma (Fig. 10a), because Bonaire is an integral part of the Dutch Antilles, and its related mantle wedge did not contaminate the melts that formed the Caribbean–Colombian Oceanic Plateau, it is shown as part of an east-dipping subduction system in the southern Caribbean (van der Lelij *et al.* 2010). At a similar time, high-pressure rocks evolved on Margarita Island and in the Venezuelan interior in the Villa de Cura allochthon (Fig. 1). Margarita appears to have been affected by subduction zone magmatism during the Aptian–Coniacian (Maresch *et al.* 2009). The blueschist-facies Villa de Cura allochthon contains some subducted slivers of island arc material of unknown protolith age, metamorphosed under barroisite-stable conditions at *c*. 96 Ma (Smith *et al.* 1999; Unger *et al.* 2005). It seems likely that both locations represent the products of subduction zone activity relatively close to the South American continent but their precise origins are uncertain.

The next event to occur, as shown in the *c*. 88 Ma reconstruction (Fig. 10b), was the formation of the felsic arc rocks of Aruba and Curaçao, which were intruded above a convergent zone through the thick basement of the Caribbean–Colombian Oceanic Plateau. This magmatism began at *c*. 88 Ma and ended with collision of the arc with South America.

Our final reconstruction covers the period between *c*. 80 and 60 Ma (Fig. 10c). Magmatism moved eastward to the Venezuelan Antilles where the Gran Roque felsic rocks formed by crustal melting at *c*. 68 to 59 Ma. Further north and east where Caribbean–Colombian Oceanic Plateau crust was absent in the Venezuelan Basin, partial melting of plume mantle and the lower crust of unknown composition contributed to formation of the Aves Ridge and La Blanquilla between *c*. 76 and *c*. 59 Ma. Spreading in the Grenada Basin (Aitken *et al.* 2010) coincides with the cessation of magmatic activity on the Aves Ridge and in the Venezuelan Antilles.

Further work is required to refine models of southern Caribbean tectonic evolution including: (1) study of the geochemistry and geochronology of igneous rocks on Tobago; (2) re-sampling of the Aves Ridge including dating of the mafic rocks; (3) detailed geochemical study of the igneous rocks of Margarita Island; (4) identification of protolith ages for the Villa de Cura allochthon; (5) a study of the link between magmatism preserved in the Dutch–Venezuelan Antilles and Villa de Cura and the Cretaceous arc rocks that have been accreted to the South American margin in Colombia and Ecuador; (6) drilling of the thin crust of the far southeastern Venezuelan Basin.

Conclusions

Dredge hauls from the SE Aves Ridge consist of subduction-related granitoids and mafic rocks. U–Pb geochronology and regional constraints indicate that they were most probably formed at *c*. 80–75 Ma. Partial melting of a plume-related mantle wedge, which lay beneath, or close to, the Caribbean–Colombian Oceanic Plateau, is believed to be the trigger for generation of the ridge. The plume-related mantle generated

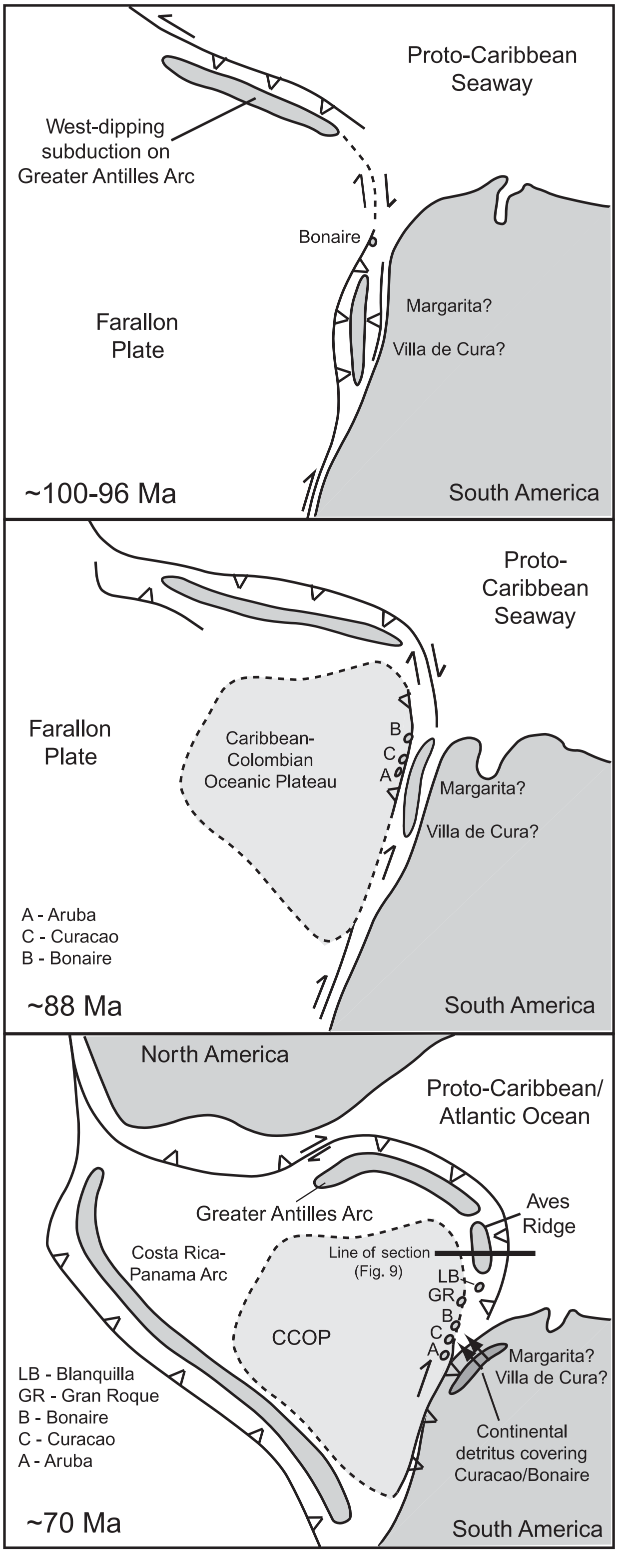

Fig. 10. Regional tectonic maps adapted from Pindell & Kennan (2009) and Wright & Wyld (2010) showing: (**a**) *c*. 100 Ma, with Bonaire as part of an east-dipping Dutch Antilles arc and Margarita and Villa de Cura close to the South American continent; (**b**) *c*. 88 Ma, with eruption of the Caribbean–Colombian Oceanic Plateau and formation of the Curaçao dykes and Aruba batholith by subduction beneath the Caribbean–Colombian Oceanic Plateau; (**c**) subduction under way beneath the Aves Ridge and Venezuelan Antilles at *c*. 75 Ma.

unusual trace element compositions identified in the mafic rocks. Island arc magmatism occurred above a subduction zone or zones separate from the SW-dipping subduction zone of the Greater Antilles arc from *c*. 88 to *c*. 59 Ma in the southern Caribbean and has been preserved as the Aves Ridge and the Dutch and Venezuelan Antilles.

I.N. acknowledges Natural Environment Research Council PhD studentship NE/F00219X/1 and NIGSFC isotope analysis grant-in-kind IP/1064/1108. R. L. Bond and G. Lozefski helped with sampling from the Lamont–Doherty Earth Observatory Deep Sea Sample Repository, supported by National Science Foundation Grant OCE00-02380/Office of Naval Research Grant N00014-02-1-0073. I. McDonald and L. Woolley assisted with major and trace element analyses. We have had valuable discussions on Caribbean tectonic evolution with J. Pindell and J. Wright. We thank J. Wright and C. Chauvel for their constructive reviews and D. Pyle for his editorial comments, which significantly improved the paper.

References

Aitken, T., Mann, P., Escalona, A. & Christeson, G.L. 2010. Evolution of the Grenada and Tobago Basins and implications for arc migration. *Marine and Petroleum Geology*, doi: 10.1016/j.marpetgeo.2009.10.003.

Bird, D.E., Hall, S.A., Casey, J.F. & Millegan, P.S. 1999. Tectonic evolution of the Grenada Basin. *In:* Mann, P. (ed.) *Caribbean Basins. Sedimentary Basins of the World, 4*. Elsevier, Amsterdam, 389–416.

Black, L.P., Kamo, S.L., Allen, C.M., Aleinikoff, J.N., Davis, D.W., Korsch, R.J. & Foudoulis, C. 2003. TEMORA 1: a new zircon standard for U–Pb geochronology. *Chemical Geology*, **200**, 155–170.

Blichert-Toft, J. 2001. On the Lu–Hf isotope geochemistry of silicate rocks. *Geostandards Newsletter*, **25**, 41–56.

Bouysse, P. 1984. The Lesser Antilles island arc: structure and geodynamic evolution. *In:* Orlofsky, S. (ed.) *Initial Reports of the Deep Sea Drilling Project, 78A*. US Government Printing Office, Washington, DC, 83–103.

Burke, K. 1988. Tectonic evolution of the Caribbean. *Annual Review of Earth and Planetary Sciences*, **16**, 210–230.

Burke, K., Fox, P.J. & Sengor, A.M.C. 1978. Buoyant ocean floor and the evolution of the Caribbean. *Journal of Geophysical Research*, **83**, 3949–3954.

Chappell, B.W., White, A.J.R. & Wyborn, D. 1987. The importance of residual source material (restite) in granite petrogenesis. *Journal of Petrology*, **28**, 1111–1138.

Christeson, G.L., Mann, P., Escalona, A. & Aitken, T.J. 2008. Crustal structure of the Caribbean–northeastern South America arc–continent collision zone. *Journal of Geophysical Research*, **113**, B08104, doi:10.1029/2007JB005373.

Church, R.E. & Allison, K.R. 2004. The petroleum potential of the Saba Bank area, Netherlands Antilles. *Search and Discovery*, Article 10076.

Clark, T.F., Korgen, B.J. & Best, D.M. 1978. Heat flow in the eastern Caribbean. *Journal of Geophysical Research*, **83**, 5883–5891.

Diebold, J.B., Stoffa, P.L., Buhl, P. & Truchan, M. 1981. Venezuelan Basin crustal structure. *Journal of Geophysical Research*, **86**, 7901–7923.

Drummond, M.S. & Defant, M.J. 1990. A model for trondhjemite–tonalite–dacite genesis and crustal growth via slab melting: Archean to modern comparison. *Journal of Geophysical Research*, **95**, 21503–21521.

Drummond, M.S., Defant, M.J. & Kepezhinskas, P.K. 1996. Petrogenesis of slab-derived trondjemite–tonalite–dacite/adakite magmas. *Transactions of the Royal Society of Edinburgh: Earth Sciences*, **87**, 205–215.

Escuder Viruete, J., Díaz de Neira, A., *et al.* 2006. Magmatic relationships and ages of Caribbean island arc tholeiites, boninites and related felsic rocks, Dominican Republic. *Lithos*, **90**, 161–186.

Escuder Viruete, J., Pérez-Estaún, A., Weis, D. & Friedman, R. 2010. Geochemical characteristics of the Río Verde Complex, Central Hispaniola: Implications for the palaeotectonic reconstructions of the Lower Cretaceous Caribbean island arc. *Lithos*, **114**, 168–185.

Fitton, J.G., Saunders, A.D., Norry, M.J., Hardarson, B.S. & Taylor, R.N. 1997. Thermal and chemical structure of the Iceland plume. *Earth and Planetary Science Letters*, **153**, 197–208.

Fox, P.J., Shreiber, E. & Heezen, B.C. 1971. The geology of the Caribbean crust: Tertiary sediments, granitic and basic rocks from the Aves Ridge. *Tectonophysics*, **12**, 89–109.

Giunta, G., Beccaluva, L., Coltorti, M., Siena, F. & Vaccaro, C. 2002. The southern margin of the Caribbean Plate in Venezuela: tectono-magmatic setting of the ophiolitic units and kinematic evolution. *Lithos*, **63**, 19–40.

Gnos, E., Kurz, D. & Eggenberger, U. 2006. Electrodynamic disaggregation of geologic material. *In: Abstracts of the 4th Swiss Geoscience Meeting, Bern, 24–25 November, 2006*. World Wide Web Address: http://geoscience-meeting.scnatweb.ch/sgm2006/index.html.

Hastie, A.R., Kerr, A.C., Pearce, J.A. & Mitchell, S.F. 2007. Classification of altered island arc rocks using immobile trace elements: development of the Th–Co discrimination diagram. *Journal of Petrology*, **48**, 2341–2357.

Hastie, A.R. 2009. Is the Cretaceous primitive island arc (PIA) series in the circum-Caribbean region geochemically analogous to the modern island arc tholeiite (IAT) series? *In:* James, K.H., Lorente, M.A. & Pindell, J.L. (eds) *The Origin and Evolution of the Caribbean Plate*. Geological Society, London, Special Publications, **328**, 397–409.

Hastie, A.R. & Kerr, A.C. 2010. Mantle plume or slab window?: Physical and geochemical constraints on the origin of the Caribbean oceanic plateau. *Earth-Science Reviews*, **98**, 283–293.

Hastie, A.R., Kerr, A.C., Mitchell, S.F. & Millar, I.L. 2008. Geochemistry and petrogenesis of Cretaceous oceanic plateau lavas in eastern Jamaica. *Lithos*, **101**, 323–343.

Hastie, A.R., Kerr, A.C., Mitchell, S.F. & Millar, I.L. 2009. Geochemistry and tectonomagmatic significance of lower Cretaceous island arc lavas from the Devil's Racecourse Formation, eastern Jamaica. *In:* James, K.H., Lorente, M.A. & Pindell, J.L. (eds) *The Origin and Evolution of the Caribbean Plate*. Geological Society, London, Special Publications, **328**, 337–359.

Hastie, A.R., Ramsook, R., Mitchell, S.F., Kerr, A.C., Millar, I.L. & Mark, D.F. 2010. Age and geochemistry of compositionally distinct back-arc basin lavas, implications for the tectonomagmatic evolution of the Caribbean plate. *Journal of Geology*, **118**, 655–676.

Hauff, F., Hoernle, K., Tilton, G., Graham, D.W. & Kerr, A.C. 2000. Large volume recycling of oceanic lithosphere over short time scales: geochemical constraints from the Caribbean Large Igneous Province. *Earth and Planetary Science Letters*, **174**, 247–263.

Haxby, W.F., Melkonian, A.K., Coplan, J., Chan, S.-M. & Ryan, W.B.F. 2010. *GeoMapApp freeware software, v.2.3*. Lamont–Doherty Earth Observatory, Palisades, NY.

Hole, M.J., Saunders, A.D., Marriner, G.F. & Tarney, J. 1984. Subduction of pelagic sediments: implications for the origin of Ce-anomalous basalts from the Mariana Islands. *Journal of the Geological Society, London*, **141**, 453–472.

Kempton, P.D. 1995. *Common Pb chemical procedures for silicate rocks and minerals, methods of data correction and an assessment of data quality at the NERC Isotope Geosciences Laboratory*. NIGL Report Series, **78**.

Kerr, A.C., Tarney, J., Marriner, G.F., Klaver, G.T., Saunders, A.D. & Thirlwall, M.F. 1996. The geochemistry and petrogenesis of the late-Cretaceous picrites and basalts of Curaçao, Netherlands Antilles: a remnant of an oceanic plateau. *Contributions to Mineralogy and Petrology*, **124**, 29–43.

Kerr, A.C., White, R.V., Thompson, P.M.E., Tarney, J. & Saunders, A.D. 2003. No oceanic plateau—no Caribbean Plate? The seminal role of an oceanic plateau in Caribbean plate evolution. *In:* Bartonlini, C., Buffler, R.T. & Blickwede, J.F. (eds) *The Circum-Gulf of Mexico and the Caribbean; Hydrocarbon Habitats, Basin Formation and Plate Tectonics*. American Association of Petroleum Geologists, Memoirs, **79**, 126–168.

Kerr, A.C., Pearson, D.G. & Nowell, G.M. 2009. Magma source evolution beneath the Caribbean oceanic plateau: new insights from elemental and Sr–Nd–Pb–Hf isotopic studies of ODP Leg 165 Site 1001 basalts. *In:* James, K.H., Lorente, M.A. & Pindell, J.L. (eds) *The Origin and Evolution of the Caribbean Plate*. Geological Society, London, Special Publications, **328**, 809–827.

Klein, M., Stosch, H.-G., Seck, H.A. & Shimizu, N. 1997. Experimental partitioning of high field strength and rare earth elements between clinopyroxene and garnet in andesitic to tonalitic systems. *Geochimica et Cosmochimica Acta*, **64**, 99–115.

Ludwig, K.R. 1999. *User's manual for Isoplot/Ex, Version 2.10, a geochronological toolkit for Microsoft Excel*. Berkeley Geochronology Center Special Publications, **1a**.

Ludwig, K.R. 2000. *SQUID 1.00, A User's Manual*. Berkeley Geochronology Center Special Publications, **2**.

MacDonald, W.D. 1968. Communication. *In*: *Status of geological research in the Caribbean 14: Mayaqüez, Puerto Rico, University of Puerto Rico*, **40**.

Maresch, W.V., Kluge, R., Baumann, A., Krückhans-Lueder, G., Pindell, J., Stanek, K. & Stöckhert, B. 2009. The occurrence and timing of high-pressure metamorphism on Margarita Island, Venezuela: a constraint on Caribbean–South America interaction. *In:* James, K.H., Lorente, M.A. & Pindell, J.L. (eds) *The Origin and Evolution of the Caribbean Plate*. Geological Society, London, Special Publications, **328**, 705–741.

Marlowe, J.I. 1968. Geological reconnaissance of parts of Aves Ridge. *In:* Manson, P. (ed.) *Abstracts of Papers from the 5th Caribbean Geological Conference, Queens College, City University of New York*, 51–52.

Mauffret, A. & Leroy, S. 1997. Seismic stratigraphy and structure of the Caribbean igneous province. *Tectonophysics*, **283**, 61–104.

McDonald, I. & Viljoen, K.S. 2006. Platinum-group element geochemistry of mantle eclogites: a reconnaissance study of xenoliths from the Orapa kimberlite, Botswana. *Applied Earth Science Transactions of the Institute of Mining and Metallurgy (B)*, **115**, 81–93.

McDonough, W.F. & Sun, S.-S. 1995. The composition of the Earth. *Chemical Geology*, **120**, 223–254.

Münker, C., Weyer, S., Scherer, E. & Mezger, K. 2001. Separation of high field strength elements (Nb, Ta, Zr, Hf) and Lu from rock samples for MC-ICPMS measurements. *Geochemistry, Geophysics, Geosystems*, **2**, 2001GC000183.

Neill, I., Gibbs, J.A., Hastie, A.R. & Kerr, A.C. 2010. Origin of the volcanic complexes of La Désirade, Lesser Antilles: implications for tectonic reconstruction of the Late Jurassic to Cretaceous Pacific–proto-Caribbean margin. *Lithos*, **120**, 407–420, doi:10.1016/j.lithos.2010.08.026.

Niu, Y., O'Hara, M.J. & Pearce, J.A. 2003. Initiation of subduction zones as a consequence of lateral compositional buoyancy contrast within the lithosphere: a petrological perspective. *Journal of Petrology*, **44**, 851–866.

Nowell, G.M. & Parrish, R.R. 2001. Simultaneous acquisition of isotope compositions and parent/daughter ratios by non-isotope dilution solution-mode plasma ionisation multi-collector mass spectrometry (PIMMS). *In:* Holland, G. & Tanner, S.D. (eds) *Plasma Source Mass Spectrometry—The New Millenium*. Royal Society of Chemistry, Cambridge, 298–310.

Peacock, S.M., Rushmer, T. & Thompson, A.B. 1994. Partial melting of subducting oceanic crust. *Earth and Planetary Science Letters*, **121**, 227–244.

Pearce, J.A. 1983. Role of the sub-continental lithosphere in magma genesis at active continental margins. *In:* Hawkesworth, C.J. & Norry, M.J. (eds) *Continental Batholiths and Mantle Xenoliths*. Shiva, Nantwich, 230–249.

Pearce, J.A. & Parkinson, I.J. 1993. Trace element models for mantle melting: application to volcanic arc petrogenesis. *In:* Pritchard, H.M., Alabaster, T., Harris, N.B.W. & Neary, C.R. (eds) *Magmatic Processes and Plate Tectonics*. Geological Society, London, Special Publications, **76**, 373–403.

Pearce, J.A. & Peate, D.W. 1995. Tectonic implications of the composition of volcanic arc magmas. *Annual Review of Earth and Planetary Sciences*, **23**, 251–285.

Pearce, J.A. & Stern, R.J. 2006. Origin of back-arc basin magmas: trace element and isotopic perspectives. *In:* Christie, D.M., Fisher, C.R., Lee, S.-M. & Givens, S. (eds) *Back-arc Spreading Systems: Geological, Biological, Chemical and Physical Interactions*. American Geophysical Union, Geophysical Monograph Series, **166**, 63–86.

Peccarillo, A. & Taylor, S.R. 1976. Geochemistry of Eocene calc-alkaline volcanic rocks from the Kastamonu area, Northern Turkey. *Contributions to Mineralogy and Petrology*, **58**, 63–81.

Petford, N. & Gallacher, K. 2001. Partial melting of mafic (amphibolitic) lower crust by periodic influx of basaltic magma. *Earth and Planetary Science Letters*, **193**, 483–499.

Petford, N., Cruden, A.R., McCaffrey, K.J.W. & Vigneresse, J.-L. 2000. Granite magma formation, transport and emplacement in the Earth's crust. *Nature*, **408**, 669–673.

Pindell, J.L. & Barrett, S.F. 1990. Geological evolution of the Caribbean region: a plate tectonic perspective. *In:* Dengo, G. & Case, J.E. (eds) *The Caribbean Region*. Geological Society of America, The Geology of North America, **H**, 405–432.

Pindell, J.L. & Kennan, L. 2009. Tectonic evolution of the Gulf of Mexico, Caribbean and northern South America in the mantle reference frame: an update. *In:* James, K.H., Lorente, M.A. & Pindell, J.L. (eds) *The Origin and Evolution of the Caribbean Plate*. Geological Society, London, Special Publications, **328**, 1–55.

Pindell, J.L., Kennan, L., Stanek, K.P., Maresch, W.V. & Draper, G. 2006. Foundations of Gulf of Mexico and Caribbean evolution: eight controversies resolved. *Geologica Acta*, **4**, 303–341.

Plank, T. 2005. Constraints from thorium/lanthanum on sediment recycling at subduction zones and the evolution of the continents. *Journal of Petrology*, **46**, 921–944.

Priem, H.N.A., Beets, D.J., Boelrijk, N.A.I.M. & Hebeda, E.H. 1986. On the age of the late Cretaceous tonalitic/gabbroic batholith on Aruba, Netherlands Antilles (southern Caribbean borderland). *Geologie en Mijnbouw*, **65**, 247–265.

Rapp, R.P. & Watson, E.B. 1995. Dehydration melting of metabasalt at 8–32 kbar: implications for continental growth and crust–mantle recycling. *Journal of Petrology*, **36**, 891–931.

Rapp, R.P., Shimizu, N., Norman, M.D. & Applegate, G.S. 1999. Reaction between slab-derived melt and peridotite in the mantle wedge: experimental constraints at 3.8 GPa. *Chemical Geology*, **160**, 335–356.

Rapp, R.P., Shimizu, N. & Norman, M.D. 2003. Growth of early continental crust by partial melting of eclogite. *Nature*, **425**, 605–608.

Royse, K.R., Kempton, P.D. & Darbyshire, F.D. 1998. *Procedure for the analysis of rubidium–strontium and samarium–neodymium isotopes at the NERC Isotope Geosciences Laboratory*. NIGL Report Series, **121**.

Salters, V.J.M., Longhi, J.E. & Bizimis, M. 2002. Near mantle solidus trace element partitioning at pressures up to 3.4 GPa. *Geochemistry, Geophysics, Geosystems*, **3**, doi:10.1029/2001GC000148.

Saunders, A.D., Tarney, J. & Weaver, S.D. 1980. Transverse geochemical variations across the Antarctic Peninsula: implications for the genesis of calc-alkaline magmas. *Earth and Planetary Science Letters*, **46**, 344–360.

Seewald, J.S. & Seyfried, W.E. 1990. The effect of temperature on metal mobility in subseafloor hydrothermal systems: constraints from basalt alteration experiments. *Earth and Planetary Science Letters*, **101**, 388–403.

Sinton, C.W., Duncan, R.A., Storey, M., Lewis, J. & Estrada, J.J. 1998. An oceanic flood basalt province within the Caribbean plate. *Earth and Planetary Science Letters*, **155**, 221–235.

Smith, C.A., Sisson, V.B., Avé Lallemant, H.G. & Copeland, P. 1999. Two contrasting pressure–temperature–time paths in the Villa de Cura blueschist belt, Venezuela: possible evidence for Late Cretaceous initiation of subduction in the Caribbean. *Geological Society of America Bulletin*, **111**, 831–848.

Speed, R.C. & Walker, B.M. 1991. Oceanic crust of the Grenada Basin in the southern Lesser Antilles arc platform. *Journal of Geophysical Research*, **96**, 3835–3852.

Stanek, K.P., Maresch, W.V. & Pindell, J. 2009. The geotectonic story of the northwestern branch of the Caribbean arc: implications from structural and geochronological data of Cuba. *In:* James, K.H., Lorente, M.A. & Pindell, J.L. (eds) *The Origin and Evolution of the Caribbean Plate*. Geological Society, London, Special Publications, **328**, 361–398.

Stephens, W.E. 2001. Polycrystalline amphibole aggregates (clots) in granites as potential I-type restite: an ion microprobe study of rare-earth distributions. *Australian Journal of Earth Sciences*, **48**, 591–601.

Su, B. 2008. Natural evidence for the garnet–spinel transition (GST) in the Earth's mantle. *Nature Proceedings*, doi:10.1038/npre.2008.1898.2.

Sun, S.-S. & McDonough, W.F. 1989. Chemical and isotopic systematics of oceanic basalts: implications for mantle composition and processes. *In:* Saunders, A.D. & Norry, M.J. (eds) *Magmatism in the Ocean Basins*. Geological Society, London, Special Publications, **42**, 313–345.

Thirlwall, M.F., Smith, T.E., Graham, A.M., Theodorou, N., Hollings, P., Davidson, J.P. & Arculus, R.J. 1994. High field strength element anomalies in arc lavas: source or process? *Journal of Petrology*, **35**, 819–838.

Thompson, P.M.E., Kempton, P.D., *et al.* 2003. Hf–Nd isotope constraints on the origin of the Cretaceous Caribbean plateau and its relationship to the Galapagos plume. *Earth and Planetary Science Letters*, **217**, 59–75.

Thompson, P.M.E., Kempton, P.D., White, R.V., Saunders, A.D., Kerr, A.C., Tarney, J. & Pringle, M.S. 2004. Elemental, Hf–Nd isotopic and geochronological constraints on an island arc sequence associated with the Cretaceous Caribbean plateau: Bonaire, Dutch Antilles. *Lithos*, **74**, 91–116.

Turner, S.P., George, R.M.M., Evans, P.J., Hawkesworth, C.J. & Zellmer, G.F. 2000. Time-scales of magma formation, ascent and storage beneath subduction-zone volcanoes. *Philosophical Transactions of the Royal Society of London, Series A*, **358**, 1443–1464.

Unger, L.M., Sisson, V.B. & Avé Lallemant, H.G. 2005. Geochemical evidence for island-arc origin of the Villa de Cura blueschist belt, Venezuela. *In:* Avé Lallemant, H.G. & Sisson, V.B. (eds) *Caribbean–South American Plate Interactions, Venezuela*. Geological Society of America, Special Papers, **394**, 223–249.

van der Lelij, R., Spikings, R.A., Kerr, A.C., Kounov, A., Cosca, M., Chew, D. & Villagomez, D. 2010. Thermochronology and tectonics of the Leeward Antilles: evolution of the Southern Caribbean Plate Boundary Zone. *Tectonics*, **29**, TC6003, doi:10.1029/2009TC002654.

Veizer, J. 1989. Strontium isotopes in seawater through time. *Annual Review of Earth and Planetary Sciences*, **17**, 141–167.

Wadge, G. & Macdonald, R. 1985. Cretaceous tholeiites of the northern continental margin of South America: the San Souci Formation of Trinidad. *Journal of the Geological Society, London*, **142**, 297–308.

Walker, B.M., Vogel, T.A. & Ehrlich, R. 1972. Petrogenesis of oceanic granites from the Aves Ridge in the Caribbean Basin. *Earth and Planetary Science Letters*, **15**, 133–139.

Wendt, J.I., Regelous, M., Collerson, K.D. & Ewert, A. 1997. Evidence for a contribution from two mantle plumes to island-arc lavas from northern Tonga. *Geology*, **25**, 611–614.

White, W.M. & Patchett, J. 1984. Hf–Nd–Sr isotopes and incompatible element abundances in island arcs: implications for magma origins and crust–mantle evolution. *Earth and Planetary Science Letters*, **67**, 167–185.

White, R.V., Tarney, J., Kerr, A.C., Saunders, A.D., Kempton, P.D., Pringle, M.S. & Klaver, G.T. 1999. Modification of an oceanic plateau, Aruba, Dutch Caribbean: implications for the generation of continental crust. *Lithos*, **46**, 43–68.

Williams, I.S. 1998. U–Th–Pb geochronology by ion microprobe. *In:* McKibben, M.A., Shanks, W.C., III & Ridley, W.I. (eds) *Applications of Microanalytical Techniques to Understanding Mineralizing Processes*. Reviews in Economic Geology, **7**, 1–35.

Wright, J.E. & Wyld, S.J. 2010. Late Cretaceous subduction initiation on the southern margin of the Caribbean plateau: one great arc of the Caribbean or three? *Geosphere* (in press).

Received 20 April 2010; revised typescript accepted 13 September 2010.
Scientific editing by David Pyle.